EVALUATION OF DUCTILE TEARING FOR API-5L X70 PIPELINE GRADE STEEL USING SENT SPECIMENS

N. Ohms[1], D. Belato Rosado[1] and W. De Waele[1]

[1] Ghent University, Laboratory Soete, Belgium

Abstract: Pipelines in harsh environments may be subjected to large deformations. Classic stress-based design needs to be complemented with strain-based design. An important parameter in the design is the crack growth resistance. SENT testing (Single Edge Notch Tension) allows to determine the so-called material’s tearing resistance curve. Very recently the first standard on SENT testing, BS 8571:2014, has been published. SENT testing is however still subject to extensive research and different approaches with respect to eg. notch placement, crack extension measurement and analysis exist. In this paper two methods for calculating crack extension based on the unloading compliance procedure are used and compared, proving that they show little difference. This is performed on an API-5L X70 steel grade and this for different configurations, namely an inner diameter notch and a through thickness notch. The results showed little difference between the different configurations, although the inner diameter showed higher crack growth resistance. Furthermore, the results are compared to visual observations of the fracture surfaces and a hardness map. The fracture surfaces corresponded to the obtained resistance curves. However, no real correlation between the hardness map and the other results could be seen.

Keywords: SENT; Unloading Compliance; resistance curves; CTOD; crack growth

1 INTRODUCTION

The continuously growing world energy demand requires access to remote resources. The pipelines to these locations have to traverse through harsh environments and may be subjected to plastic deformation while in service due to imposed displacements. A strain-based approach is needed in the design of such pipelines.

In strain-based design, the longitudinal strain capacity, in addition to transverse yield strength is used as a measure for design safety. An important parameter in this design is the crack growth resistance [1].

Single edge notch tension testing (SENT) is a good laboratory scale test to evaluate the tearing resistance of pipelines with defects. The unloading compliance method allows accurate measurement of crack growth and the development of a crack growth resistance using a single specimen [2]. Several analytical equations have been developed to calculate the crack growth based on the measured specimen compliance. In this article, two equations will be compared. SENT specimens are extracted from an API-5L X70 pipeline steel grade and defects are introduced in the base metal at different locations. Differences in the calculated resistance curves will be compared to the visual information on the fracture surfaces and to a hardness map.

2 UNLOADING COMPLIANCE

2.1 Procedure

The resistance against ductile crack growth extension is characterized by so-called tearing resistance curves or R-curves. These express the fracture toughness as J-integral or CTOD (Crack Tip Opening Displacement) values against ductile crack extension. From this, the crack driving force for a certain amount of ductile tearing to occur can be obtained.

One way to obtain the ductile crack extension from a SENT test is the unloading compliance technique, which is described by Shen et al. [3]. This method is based on the measurement of the specimen’s compliance *C*. This compliance is the inverse of the specimen’s stiffness and is expressed in mm/kN (see eq.1). It is assumed that there is a direct relationship between the compliance and the crack dimensions. An increase in compliance indicates crack growth.

$$C = \frac{\Delta CMOD}{\Delta F} \qquad (1)$$

In this equation *CMOD* is the crack mouth opening displacement, which can be obtained by using a double clip-gauge setup as described by Verstraete et al. [4]. *F* is the force exerted on the specimen and can be measured by a load cell in the test rig.

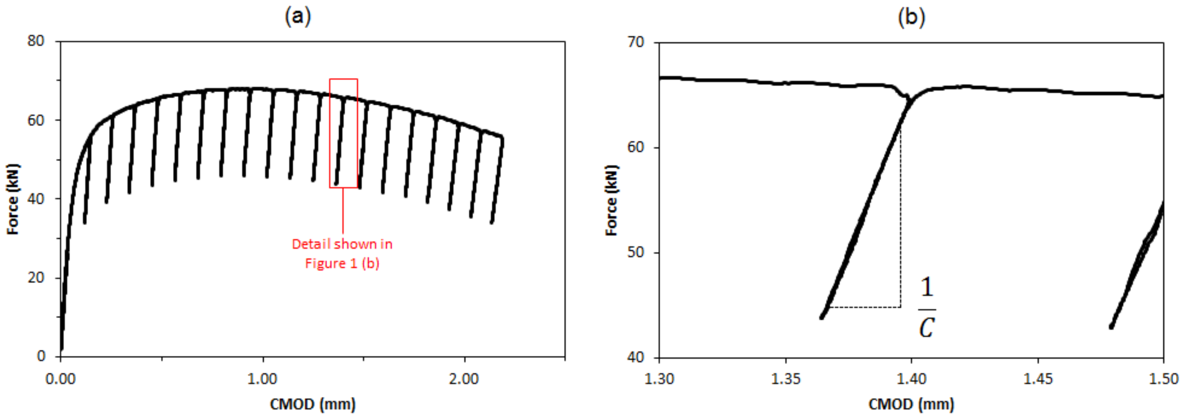

Figure 1. Example of unloading compliance curve (a) and detail of unloading cycle (b).

The unloading compliance method periodically loads and unloads the specimen at predefined *CMOD* intervals. At the beginning of the test, the specimen is loaded and unloaded several times in the elastic zone at a fixed load. After this, the specimen has loading/unloading cycles at a fixed *CMOD* increase. Following maximum load, the test is stopped when a load is reached that equals 80% of this maximum. The typical evolution of load versus *CMOD* during such a test is displayed in Figure 1 (a). Figure 1 (b) shows a detail of one unloading cycle from which the compliance is calculated.

The crack size can be calculated from the elastic unloading using the following nth-order polynomial:

$$a/W = \sum_{i=0}^{n} r_i U^i \qquad (2)$$

In equation (2), *a/W* represents the crack size *a* normalized to the specimen width *W*. *U* is a dimensionless parameter which can be calculated using the next equation:

$$U = \frac{1}{1+\sqrt{B_e C E}} \qquad (3)$$

Here, B_e is the effective specimen thickness as recommended in ASTM E 1820 [5], *C* is the obtained compliance and *E* Young's modulus.

There are many reports which make use of equation (2), although there are different definitions for the polynomial. They mainly differ in the order of the polynomial and the used coefficients r_i. Determining factors are among others the daylight gripping length *H* (specimen length between the gripping points), width-to-thickness ratio (*W/B*) and fixing method.

Shen et al. [6] showed that a daylight gripping length of *H=10W* gives a good similarity towards a circumferential crack in a pipe subjected to tensile loading. Preferably, the width should be taken equal to the thickness (*W=B*) [7]. Two used gripping methods are pin-loaded and clamped. The clamped method is preferred because it gives better defined boundary conditions and the pin-loaded method is influenced by the pin location [2], [8].

Table 1. Assumptions of the *CMOD* based compliance equations.

Cravero (2007)	Shen (2009)
H=10W	H=10W
5th order polynomial	8th order polynomial
Clamped	Clamped
Not specified	W=B
Plane strain	Plane stress
$E' = E/(1-\nu^2)$	E
0.1≤a/W≤0.7	0.05≤a/W≤0.95

Wang et al. [9] determined that there are six *CMOD* based compliance equations in the form of equation (2) which use the aforementioned configurations. They concluded that the two most accurate equations are given by Cravero et al. [10] and by Shen et al. [2]. Although both equations have the form of equation (2), they are both based on different assumptions. The most important are given in Table 1.

The first difference between the two is that Cravero assumes a plane strain state of the specimen whereas Shen assumes a plane stress state. As a result different definitions of the Young's modulus *E* in equation (2) are used. For plane stress, the conventional modulus *E* is used. For plane strain on the other hand, the elastic modulus corresponding to plane strain *E'* is used. *E'* is the normal elastic modulus *E* corrected by Poisson's ratio *v*. Although the material is at a plane strain condition at the center, the sides are in a plane stress condition. Since the compliance is a function of displacements everywhere in the specimen and not just around the crack tip, Tyson et al. [11] concluded that it is best to use the plane stress condition, because the constraint for the major part of specimens in tension is closer to plane stress.

A second difference lies in the order of the polynomial and accompanying coefficients r_i. The values for the coefficients r_i are given in Table 2. These values are independent of the width-to-thickness ratio, the relative crack depth *a/W* or the assumed state (plane stress or plane strain).

Table 2. Coefficients r_i for equation (2) .

	r_0	r_1	r_2	r_3	r_4	r_5	r_6	r_7	r_8
Cravero	1.6485	-9.1005	33.025	-78.467	97.344	-47.277			
Shen	2.072	16.411	79.600	-211.670	236.857	27.371	-179.740	-86.280	171.764

A third difference lies in the applicability area where the polynomial is accurate. The 5th order polynomial is valid for values of *a/W* between 0.1 and 0.7. The 8th order polynomial, although more cumbersome, does have a larger interval of validity ($0.05 \le a/W \le 0.95$). A comparative study performed by Tyson et al. [11], determined a very small difference between the two definitions in an interval of $0.1 \le a/W \le 0.8$. Wang et al. [9] also noted a small difference between the two methods, although they concluded that the 5th order polynomial as proposed by Cravero was the most precise.

The *CTOD* can be calculated using the double clip gauge setup and the 90° intercept. Both are defined by Verstraete et al. [4]. The obtained values should then be fitted according to the following equation, which is defined by ASTM E 1820 [5]:

$$CTOD = \alpha_\delta (\Delta a)^{\eta_\delta} \qquad (4)$$

The term Δa is the crack growth and α_δ and η_δ are calculated coefficients according to [5].

2.2 Specimens

The materials used in this study are samples cut from a spiral formed API-5L X-70 pipeline steel grade. The specimens have been taken longitudinally to the pipe axis, which has a 25° angle to the rolling direction of the material. Two different notch configurations have been evaluated. The first notch configuration is an inner diameter (I.D.) notch and the second one is a through-thickness (T.T.) notch. According to the provisions of standard ASTM E 1820 [5], three specimens are tested for each configuration. The different configurations are shown in Figure 2 (a) and (b).

As advised by Shen et al. [12], V-shaped side grooves are applied to the specimen. These side grooves are cut at the sides of the specimen at the same location as the notch. These side grooves promote a uniform crack extension.

As discussed in paragraph 2.1, the specimens are clamped, with a daylight gripping length $H=10W$ and a square cross-section $W=B$. The initial relative crack depth a_0/W equals 0.3. This was chosen according to Moore et al. [13], who determined that an initial relative crack depth of 0.3 gives accurate *CTOD* measurement. Further characteristics of the material are given in Table 3.

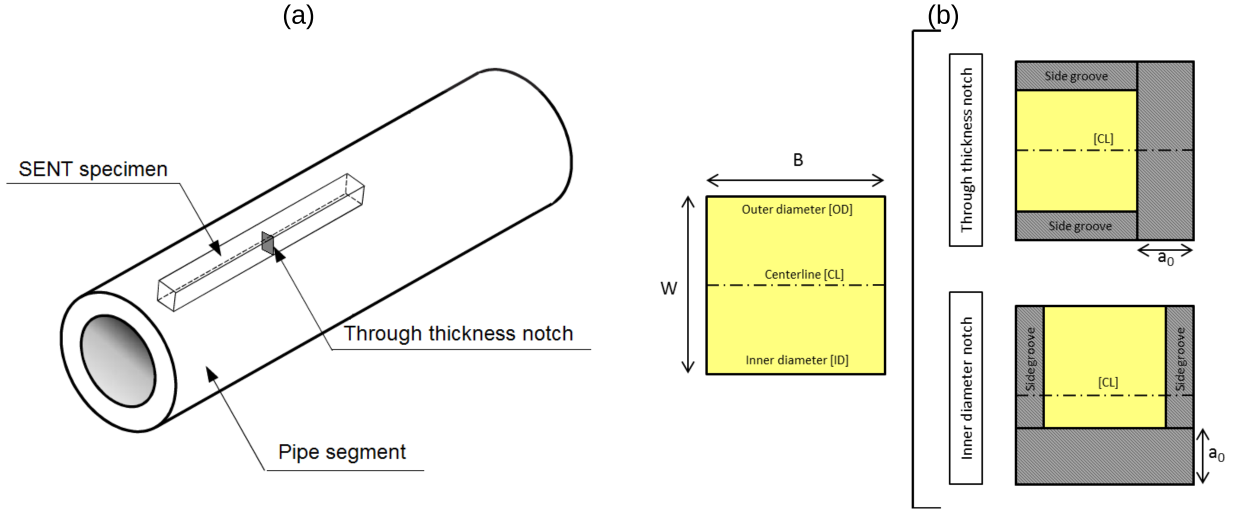

Figure 2. Specimen and TT notch orientation in pipe (a) and cross section configuration (b).

Table 3. Specimen characteristics.

Notch	W [mm]	B [mm]	a_0/W	H [mm]	σ_y [Mpa]	Specimens
T.T.	12.5	12.5	0.3	125	553	TT1 TT2 TT3
I.D.	12.5	12.5	0.3	125	553	ID1 ID2 ID3

3 TEST RESULTS

3.1 Crack growth

For the calculation of the crack growth as discussed paragraph 2.1, the methods proposed by Cravero and Shen are both used to determine *a/W* in order to see the difference between them. For all specimens evaluated, the values obtained from Shen are always lower than the values from Cravero, although these differences are minute. All differences are less than 1% of the values of Cravero. The difference between the calculated points is displayed in Figure 3. For both the TT notched and ID notched specimens it can be seen that Shen's values are always lower, but the difference gets gradually smaller for higher *a/W* values.

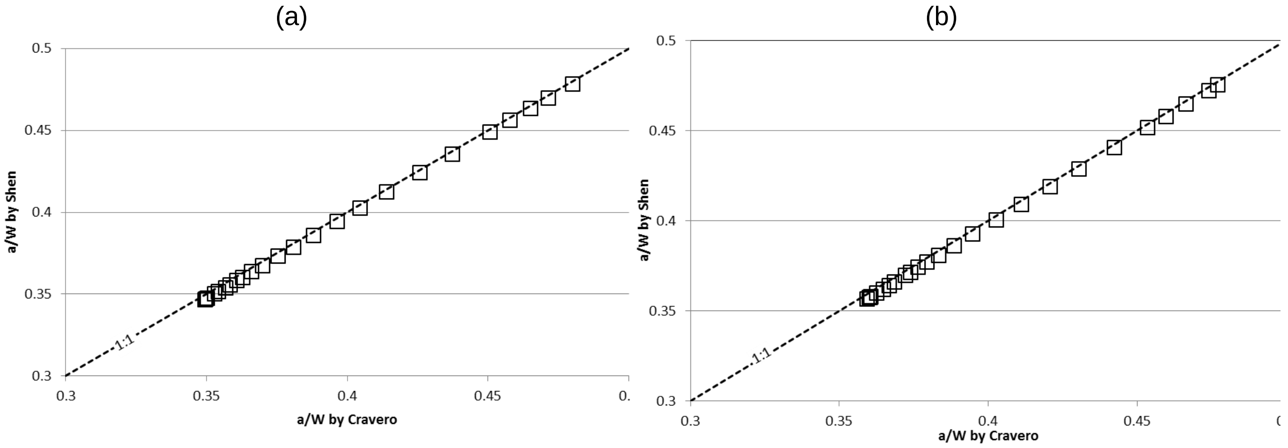

Figure 3. a/W comparsion between Cravero and Shen for TT notched specimens (a) and ID notched specimens (b).

As can be seen above, the differences are very small. This is in accordance to the observations made by Tyson et al. [11] and Wang et al. [9]. Table 4 shows a comparison between the final crack measurements; $a_{p,C}$ and $a_{p,S}$ are the final calculated crack lengths according to Cravero's and Shen's equation respectively, a_p is the measured crack length according to the nine points average method as proposed by ASTM E 1820 [5].

Table 4. Final crack length in [mm].

Specimen	$a_{p,C}$	$a_{p,S}$	a_p	$\|a_p - a_{p,C}\|$	$\|a_p - a_{p,S}\|$
TT1	5.93	5.90	5.81	0.12	0.09
TT2	5.95	5.93	5.90	0.05	0.03
TT3	6.05	6.03	5.91	0.14	0.12
ID1	5.89	5.87	5.72	0.17	0.15
ID2	5.98	5.96	5.98	0.00	0.02
ID3	5.94	5.91	5.76	0.18	0.15

From Table 4 it can be seen that the values obtained by Shen's method are in all but one case closest to the measured values (grey values). Again, the values don't differ much between the two methods.

Since the difference is small, the values of the 5th order polynomial are used for further calculations.

3.2 Resistance curves

Figure 4 displays the CTOD-R curves as determined in paragraph 2.1. Figure 4 (a) show the data points for the three through thickness notched specimens and (b) for the three inner diameter notched specimens. On both images, the final crack extension is indicated by a red dashed line. From the figures it can be seen that the inner diameter notched specimens have a slightly higher tearing resistance. The inner diameter notched specimens also have less scatter in the major part of the curve and the data points seem to coincide to a general line. For the TT notched specimens there is more scatter overall.

This higher scatter for the TT configuration and lower scatter for the ID configuration can be seen in Figure 5 (a) and (b) respectively. These data points are determined by fitting the experimental data to equation (4). It needs to be remarked that only those points that fall between an interval, which is specified in ASTM E 1820 [5], are used. The full line is the total fitting line for the three specimens. The scatter band width is determined by the 95% interval of the points lying in the previous mentioned interval. Again, on Figure 5 (b) it can be clearly seen that the data points coincide with the total fitting curve.

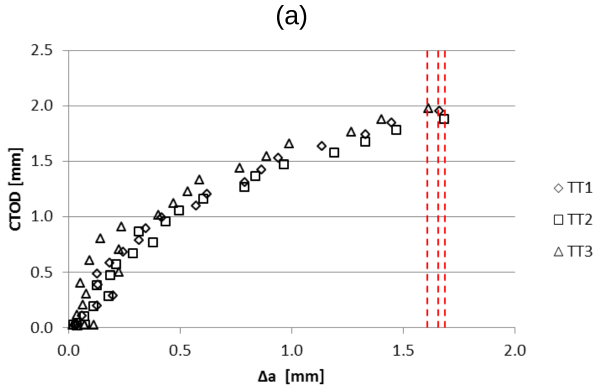

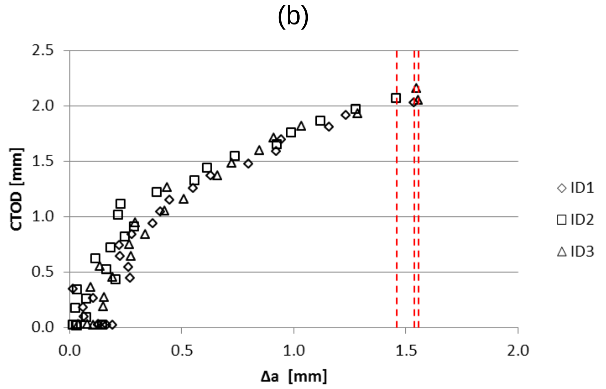

Figure 4. CTOD-R curves for the three TT notched specimens (a) and CTOD-R curves for the three ID notched specimens (b).

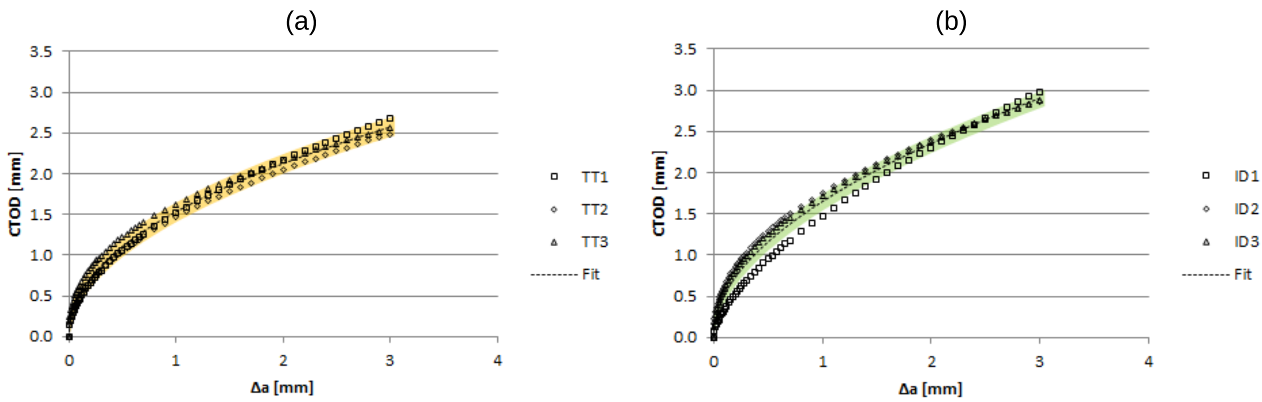

Figure 5. Fitted CTOD-R curves for the three TT notched specimens with total fit and scatter band (a) and fitted CTOD-R curves for the three ID notched specimens with total fit and scatter band.

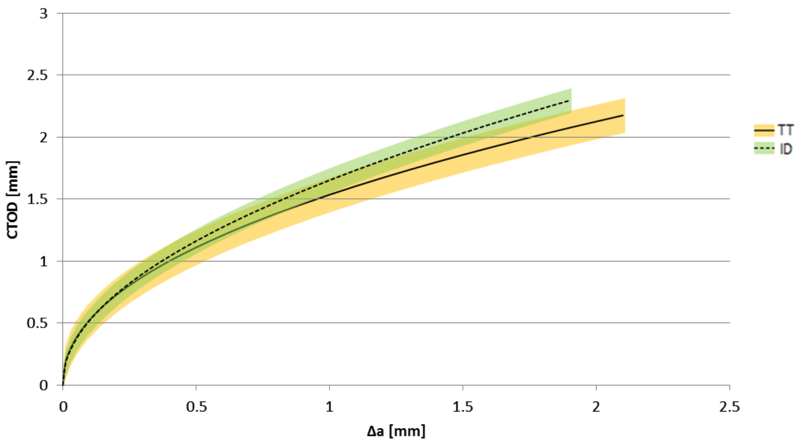

Figure 6. Fitted CTOD-R curve for TT and ID configurations with scatter band and final crack extension.

Figure 6 shows a comparison of the fitted tearing resistance curves for TT and ID configurations together with the scatter bands. The curves have been cut off at the final crack extension. From this figure it can be clearly seen that the ID specimens have a higher crack growth resistance, although this difference is small. The ID specimens also have a smaller total crack propagation. The slightly worse results for crack resistance for the TT specimens can be due to microstructural heterogeneity along the crack front. Due to the rolling process, the surfaces and the inner part of the pipe will have slightly different microstructural appearances and thus different strength and toughness properties.

3.3 Fracture surfaces

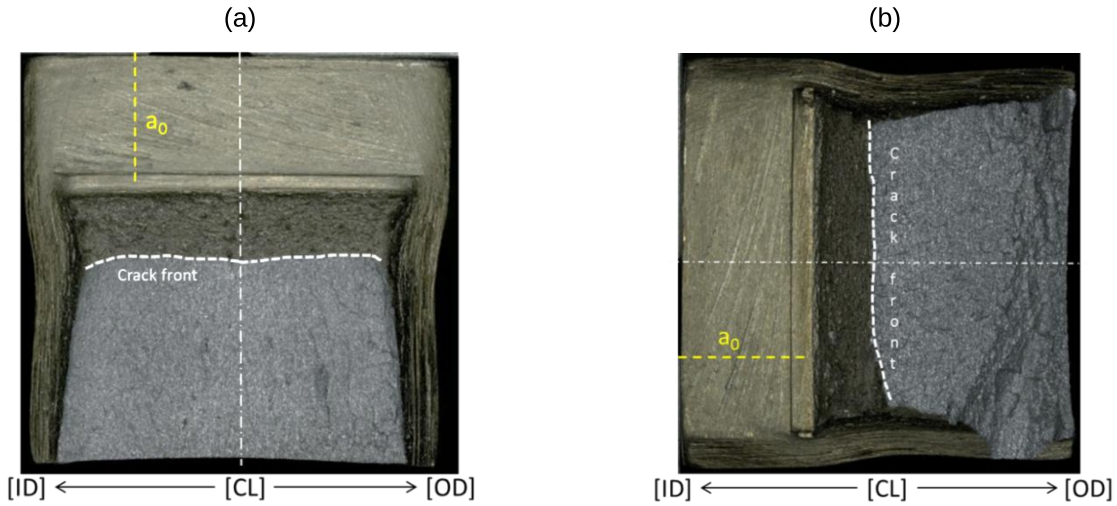

Figure 7. Fracture surface for TT notch (a), fracture surface for ID notch (b).

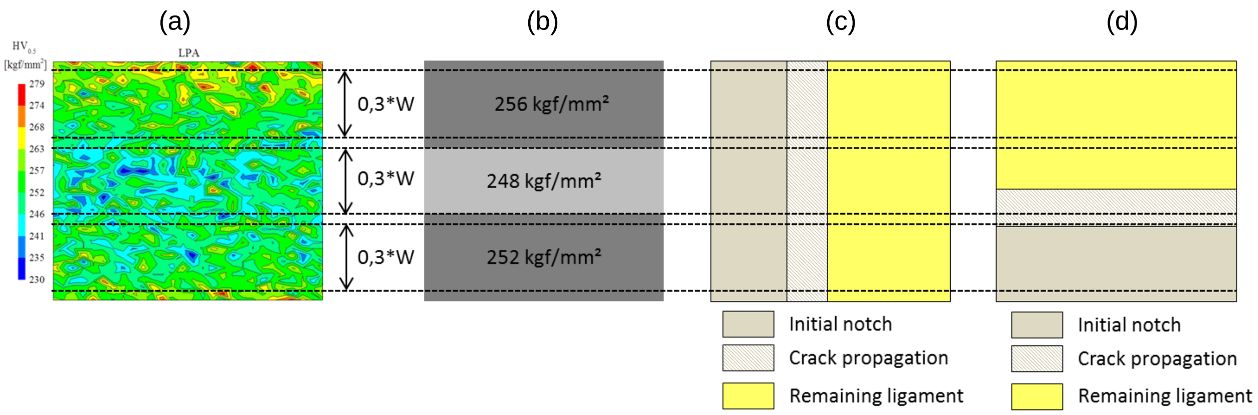

Figure 8. Vickers hardness map (a), average hardness zones (b), ductile tearing location for TT notched specimen (c) and ductile tearing location for ID notched specimen (d).

Figure 7 (a) and (b) show the fracture surfaces of one specimen for each configuration. For the TT notched specimen the crack extension appears constant, with a very slight increase at the center and on the sides. For the other TT configuration specimens, the same was seen except for the sides, which remained straight. For the ID notched specimen a certain slope in the crack front is noticeable. This slope was seen on all three specimens.

Figure 8 (a) shows the hardness map of the material which was obtained from an ongoing PhD research. On this map three regions can be identified; two outer regions with higher hardness and an inner region with lower hardness. These three regions are schematically shown with the corresponding average value in Figure 8 (b). Figure 8 (c) and (d) show how the cracks propagated through these regions for the TT and ID configurations respectively. The TT notch stands perpendicular to these zones, so as the crack propagates, the hardness doesn’t change in the forward direction. The ID notch however starts at the harder zone and propagates into the softer center region. This transition of hardness zones may explain the slightly unstable crack front.

4 CONCLUSIONS

The unloading compliance method was used to determine the crack growth in SENT specimens extracted from an X70 pipe steel grade. Several different approaches exist (although most are very similar) and two of those were used here. It was shown that these two methods show a minimal difference between the two and approach the reality well, allowing the choice of method. This was also confirmed in other literature. In this paper the shorter and less cumbersome method as proposed by Cravero was used for the calculations.

The determined CTOD-R curves showed that the material has a slightly larger crack growth resistance to inner diameter defects than through thickness defects. The through thickness specimens were also more prone to scatter, this is probably due to the heterogeneity of the material microstructure throughout the thickness.

The hardness map provides a visual insight of the varying levels of hardness, which in turn are related to microstructural heterogeneities across the section, such as grain size variations and distribution of secondary hard particles. The two notch configurations are positioned differently with regard to this heterogeneity and this may explain the difference in crack propagation and tearing resistance. Further analysis of the matter is part of an ongoing research.

5 ACKNOWLEDGEMENTS

The authors would like to acknowledge the support of Stijn Hertelé for this theoretical and technical support.

6 REFERENCES

[1] Macia, M.L., Kibey, S.A., Arslan, H., Bardi, F., Ford, S.J., Kan, W.C., Cook, M.F. and Newbury, B., 2010, “Approaches to Qualify Strain-Based Designed Pipelines”, International Pipeline Conference, Calgary, Alberta, Canada, paper n° IPC2010-31662

[2] Shen, G. W., Gianetto, J. A., and Tyson, W. R., 2009, “Measurement of J-R curves using single-specimen technique on clamped SE(T) specimen”, Proceedings of 19th International Offshore and Polar Engineering Conference, Osaka, Japan, pp92-99

[3] Shen, G., and Tyson, W. R., 2009, "Crack Size Evaluation Using Unloading Compliance in Single-Specimen Single-Edge-Notched Tension Fracture Toughness Testing", Journal of Testing and Evaluation, 37, pp. 347-357

[4] Verstraete, M., 2014, “Experimental-Numerical Evaluation of Ductile Tearing Resistance and Tensile Strain Capacity of Biaxially Loaded Pipelines”, Ph.D. thesis, Ghent University, Ghent, Belgium

[5] American Society of Testing and Materials, 2011, E1820 - Standard Test Method for Measurement of Fracture Toughness.

[6] Shen, G, Bouchard, R, Gianetto, JA, and Tyson, WR, “Fracture Toughness Evaluation of High Strength Steel Pipe”, Proceedings of PVP2008, ASME Pressure Vessel and Piping Division Conference, Chicago, Illinois, USA, PVP2008-61100

[7] ExxonMobil, 2010, "Measurement of Crack-Tip Opening Displacement (CTOD), Fracture Resistance Curves Using Single-Edge Notched Tension (SENT) Specimens"

[8] Det Norske Veritas, 2006, RP-F108: Fracture Control for Pipeline Installation Methods Introducing Cyclic Plastic Strain

[9] Wang, E., Omiya, M., 2014, “Finite Element Analysis of Crack Mouth Opening Displacement Compliance in Crack Length Evaluation for Clamped Single Edge Tension Specimens”, Fatigue & Fracture of Engineering Materials & Structures, 38, pp.315-329

[10] Cravero, S., Ruggieri, C., 2007, “Estimation procedure of J-resistance curves for SE(T) fracture specimens using unloading compliance”, Engineering Fracture Mechanics, 74, pp. 2735-2757

[11] Tyson, B., Ding, P., Wang, X., 2014, “Elastic compliance of single-edge-notched tension SE(T) (or SENT) specimens”, Frattura ed Integrità Strutturale, 30, pp. 95-100

[12] Shen, G., Tyson, W. R., Gianetto, J. A., and Park, D.-Y., 2010, "Effect of Side Grooves on Compliance, J-Integral and Constraint of Clamped SE(T) Specimen", Pressure Vessels and Piping Conference, Bellevue, Washington, USA, paper n° PVP2010-25164

[13] Moore, P. L., and Pisarski, H. G., 2012, "Validation of Methods to Determine CTOD from SENT Specimens", International Offshore and Polar Engineering Conference, Rhodes, Greece, pp. 577-582